Electronic Supplementary Information

Calcium oxalate precipitation by diffusion using laminar microfluidics: toward a biomimetic model of pathological microcalcifications

G. Laffite[ab], C. Bonhomme[b], C. Leroy[b], L. Bonhomme-Coury[b], E. Letavernier[c], M. Daudon[c], V. Frochot[c], JP Haymann[c], S. Rouzière[d], I. T. Lucas,[e] D. Bazin[bd] F. Babonneau[b] and A. Abou-Hassan*[a]

[a] Sorbonne Universités, UPMC Univ Paris 06, UMR 8234 CNRS, Laboratoire Physico-chimie des Electrolytes, Nanosystèmes Interfaciaux (PHENIX), 4 place Jussieu - case 51, F-75005, Paris, France.

[b] Sorbonne Universités, UPMC Univ Paris 06, CNRS, Collège de France, Laboratoire de Chimie de la Matière Condensée de Paris (LCMCP), 11 Place Marcelin Berthelot, Bat D, F-75005, Paris, France.

[c] Sorbonne Universités, UPMC Univ Paris 06, AP-HP, INSERM, Service d'Explorations Fonctionnelles, Hôpital Tenon, 4 rue de la Chine, 75020, Paris, France.

[d] Laboratoire de Physique des Solides, CNRS UMR 8502, Université Paris-Sud, Bât 510, 91405, Orsay, France.

[e] Sorbonne Universités, UPMC Univ Paris 06, UMR 8235 CNRS, Laboratoire Interfaces et Systèmes Electrochimiques (LISE), 4 place Jussieu – case 133, F-75005, Paris, France.

*Corresponding author: ali.abou_hassan@upmc.fr

1. Chemicals

Calcium chloride and sodium oxalate salts were respectively purchased from Merck and Prolabo and used as received.

2. Microfluidic device fabrication

The PDMS microchannels were produced using a standard soft lithographic process[1] briefly described in the following. In a first step, a rigid mold containing the "Y shaped" pattern was fabricated on a <100> oriented silicon wafer using a SU8 2100 photoresist (Micro- Chem Corp) suitable for the design of 100 µm in depth microstructures. For the mold replication, a liquid elastomer base (Sylgard, 184, Dow Corning) was manually mixed with its curing agent in a proportion of 10:1 (w/w). The mixture was then degased in a vacuum chamber during 1 h, poured on the silicon mold and cured in an oven at 65 °C during 2 h. Finally, the PDMS containing the replicated pattern was carefully peeled off from the silicon mold and holes used for liquids injection were manually punched.

3. COMSOL simulations

The distribution of calcium and oxalate species at 25°C in the channel was modelled in the convection and diffusion modes using the steady-state incompressible *Navier-Stokes* equation using the chemical engineering module of COMSOL Multiphysics 4.2.

The mass balance equation implemented in the convection and diffusion application mode is given by:

$$\nabla . \left(- D_i \nabla c_i \right) = \; - u \nabla . c_i \qquad (1)$$

where c_i is the concentration of species i ($c_{oxalate}$=12.0 mmol.L^{-1} and $c_{calcium}$=0.40 mmol.L^{-1}), D_i is the self-diffusion constants of species i at infinite dilution in water at 25°C ($D_{oxalate}$ = 9.87 x 10^{-10} m^2.s^{-1} and $D_{calcium}$ = 7.92 x 10^{-10} m^2.s^{-1} from ref [2]) and u is the velocity vector (m.s^{-1}).

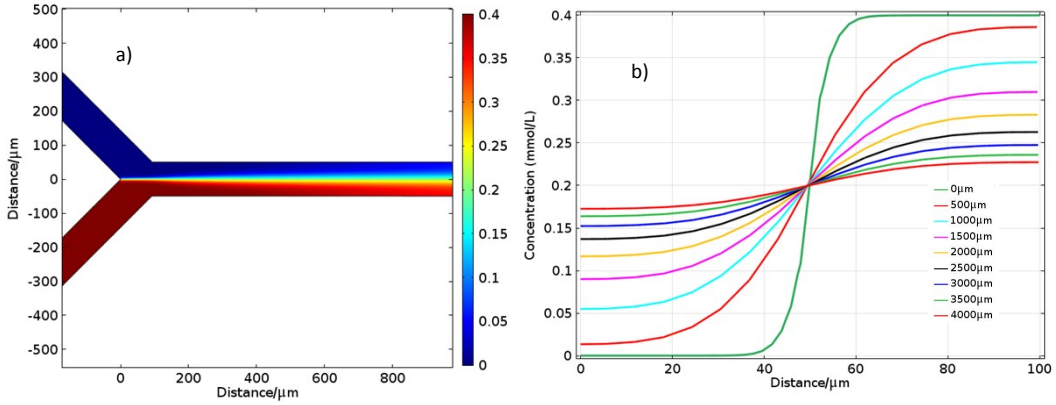

Fig. S1. Simulated calcium concentration distribution at a flow rate $Q_{calcium}$ of 1 µL.min^{-1}: concentration distribution of calcium (a) and concentration profile of calcium (b) as a function of the transverse coordinate of the microchannel at different distance away from the junction. The concentration gradient is displayed as a color gradient from 0 (blue) to 0.4 (red).

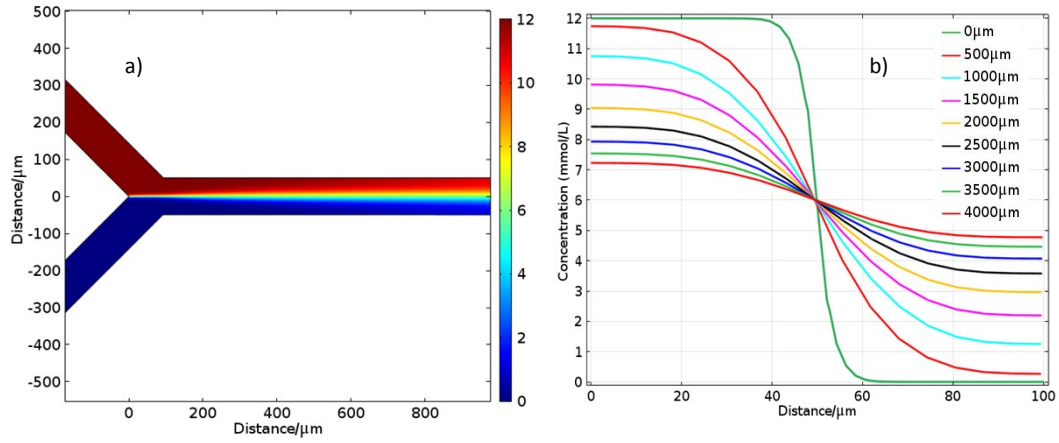

Fig. S2. Simulated oxalate concentration distribution at a flow rate $Q_{oxalate}$ of 1 µL.min^{-1}: concentration distribution of oxalate (a) and concentration profile of oxalate (b) as a function of the transverse coordinate of the microchannel at different distance away from the junction. The concentration gradient is displayed as a color gradient from 0 (blue) to 12 (red).

Finally the supersaturation (SS) gradients were also simulated in the microchannel using the following definition :[3]

$$SS = \frac{c_{oxalate} \times c_{calcium}}{c^{eq}_{oxalate} \times c^{eq}_{calcium}} \qquad (2)$$

where $c^{eq}_{oxalate}$ and $c^{eq}_{calcium}$ are the concentration of oxalate and calcium at equilibrium, respectively (*i.e* the solubility at 25°C is about 4mg/L or 3.1x10^{-2} mmol.L^{-1}).[4]

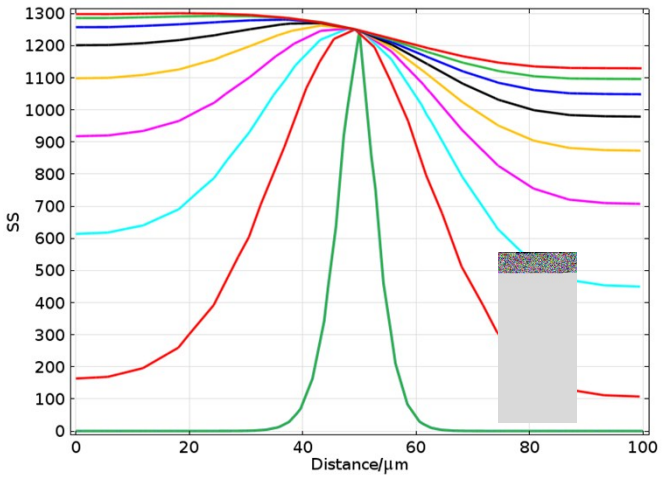

Fig. S3. Supersaturation (SS) profile distribution during mixing in the channel at flow rates $Q_{oxalate}$ and $Q_{calcium}$ of 1 µL.min^{-1} as a function of the transverse coordinate of the microchannel at different distance away from the junction.

4. Experimental

4.1 Raman scattering

Raman spectra with a 0.5 cm^{-1} spectral resolution were collected during 30s on a Labram HR800 instrument (Horiba, Japan) with a Newton EM-CCD (Andor technology, UK) using a 633nm excitation laser (1 mW) and a 100x objective (Olympus, Japan). Raman maps (80 x 60 µm) with a 2µm step were acquired under similar conditions using a 0.25 s collection time *per* pixel.

4.2 X-ray diffraction

X-ray diffraction measurements were performed on a MARdtb goniometer installed on a copper rotating anode generator with monochromatized radiation (wavelength = 1.542 Å) obtained by a multilayer W/Si optics. The microscope glass slide with the precipitated crystals was placed between the beam collimation slits and the detector. Diffraction patterns were recorded on a MAR research X-ray sensitive 345 mm plate detector with 150µm pixel size. Home-made software allows for the angular grouping of measured intensities to obtain scattering diagrams I(Q).

4.3 Infrared spectroscopy

FT-IR spectra were recorded directly on the microchannel equipped with a metallized glass slide, using a Perkin-Elmer FT-IR Frontier spectrometer coupled with a Perkin-Elmer FT-IR Spotlight 400 microscope.

5. Results

5.1 X-ray diffraction (XRD)

The observed 2D X-ray diffraction diagram in Fig. S4a reveals rings and dots, underlining the presence of quite large crystals in the microfluidic channel (as confirmed by SEM – see Fig. 2 in the main text). However, the non-flat base line observed on the spectrum in Fig. S4b is a consequence of the high scattering due to the glass slide substrate. Characteristic high intensity peaks (AU > 50 %) specific for the COM phase can be extracted for angles at 14.95 °, 24.43 °, 30.2 ° (space group P2_1/c; a=6.283Å ; b=14.560Å; c=10.116Å ; β = 109.59 °). The use of Kapton® film rather than glass slide (more suitable for XRD experiments) is currently under investigation.

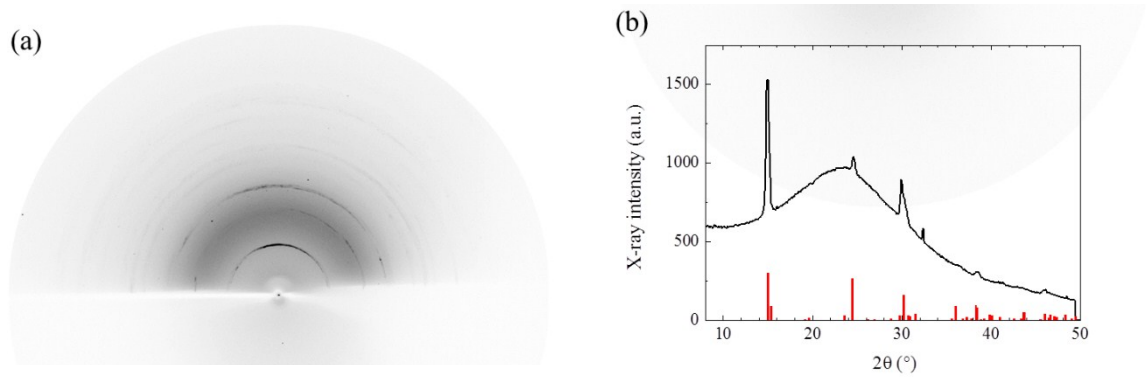

Fig S4. a) 2-D X-ray diffraction pattern of the precipitated crystals obtained on the microscope glass slide in the microfluidic device. b) Associated X-Ray diagram with characteristic peaks of COM phase, red lines indicating the tabulated values.

5.2 FT-IR experiments

FT-IR spectrum (Fig. S5a) recorded in the upper region of the microchannel where mainly only twinned crystals were observed (Fig. S2), presents weak but rather well defined bands in the 3000-3500 cm^{-1} region (ν(OH)), strong ν(C-O) bands at 1606 cm^{-1} and 1312 cm^{-1}, the out of plane bending mode of water at 776 cm^{-1} and a weak adsorption band at 883 cm^{-1} demonstrating the presence of COM phase (in agreement with the observed crystal morphology).[5] FT-IR spectrum (Fig. S5b) recorded in the lower region of the microchannel where tapered bipyramids were also present, shows much broader bands, especially in the ν(OH) region, which is characteristic of the COD phase. However the low signal-to-noise ratio prevents any definitive identification[4].

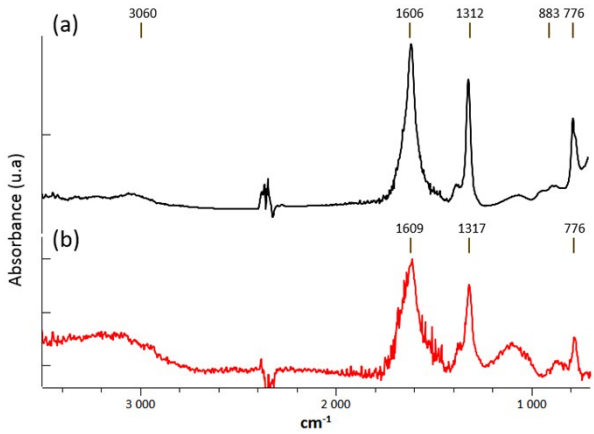

Fig. S5. ATR FT-IR spectra of precipitated crystals formed in a) the upper region and b) the lower region of the microchannel **(see Figure 2 in the main text).**

References:

1. Y. X. and and G. M. Whitesides, *Annual Review of Materials Science*, 1998, **28**, 153-184.
2. J. Buffle, Z. Zhang and K. Startchev, *Environmental Science & Technology*, 2007, **41**, 7609-7620.
3. B. Finlayson, *Kidney Int*, 1978, **13**, 344-360.
4. S. S. Atanassova and I. S. Gutzow, *Biomed. Res. Int.*, 2013, 374950.
5. P. Carmona, J. Bellanato and E. Escolar, *Biospectroscopy*, 1997, **3**, 331-346.